Analysis of Microwave Heating of Materials with Temperature-Dependent Properties

ARTICLE *in* AICHE JOURNAL · MARCH 1991

Impact Factor: 2.75 · DOI: 10.1002/aic.690370302

Reprinted from AICHE JOURNAL, March 1991

Analysis of Microwave Heating of Materials with Temperature-Dependent Properties

K. G. Ayappa and H. T. Davis
Dept. of Chemical Engineering and Materials Science, University of Minnesota, Minneapolis, MN 55455
E. A. Davis and J. Gordon
Dept. of Food Science and Nutrition, University of Minnesota, St. Paul, MN 55108

Transient temperature profiles in multilayer slabs are predicted, by simultaneously solving Maxwell's equations with the heat conduction equation, using Galerkin finite elements. It is assumed that the medium is homogeneous and has temperature-dependent dielectric and thermal properties. The method is illustrated with applications involving the heating of food and polymers with microwaves. The temperature dependence of dielectric properties affects the heating appreciably, as is shown by comparison with a constant property model.

Introduction

The use of microwaves as a source of thermal energy is rapidly growing. Brief startup times and internal heating, due to penetration of microwaves, improve the efficiency and reduce process times, making it an attractive source of thermal energy. The food industry is the largest consumer of microwave energy where it is used for cooking, thawing, tempering, freeze-drying, pasteurization, and sterilization. Microwaves are used in ceramic processing for drying and sintering (Chabinsky, 1988) and in the polymer industry to cure epoxy resins (Jow et al., 1988; Le Van et al., 1987) and process adhesives (Malaczynski, 1988). Microwave power is also employed in the drying of paper, forest products and textiles (Chabinsky, 1988).

As a result of dielectric losses, microwave absorption provides a volumetrically distributed heat source. The temperature distribution in a substance subjected to microwave radiation is thus governed by the interaction and absorption of radiation by the medium and the accompanying transport processes due to the dissipation of electrical energy into heat. Modeling power absorption patterns in objects exposed to electromagnetic radiation may have been performed most extensively in the biomedical community, where safe radiation exposure levels need to be determined for hyperthermia treatment (Durney, 1980). Maxwell's equations have been solved by finite difference, finite element and boundary element methods to obtain power deposition patterns in slabs, cylinders, spheres, and human torsos (Schwan et al., 1953, 1956; Livesay et al., 1974; Weil, 1975; Taflove and Brodwin, 1975; Neuder, 1979; Spiegel, 1984; Lynch et al., 1985). Microwave heating in bilayer tissues was studied by Guy (1971), and a coupled analysis of temperature and power distributions during hyperthermia was studied by Mandal et al. (1989).

In several computational studies of microwave heating, the heat generation in foods has been modeled by Lambert's law, in which the microwave power is attenuated exponentially as a function of distance of penetration into the sample (Datta, 1990). Lambert's law is valid for semiinfinite samples and has been used to predict temperature profiles during microwave heating (Ohlsson and Bengtsson, 1971; Stuchly and Hamid, 1972; Nykvist and Decareau, 1976; Taoukis et al., 1987; Chan et al., 1973). In a recent work, we have shown that Lambert's law can be used for samples thicker than about three times the characteristic penetration depth of microwaves, but the law fails for thinner samples (Ayappa et al., 1990). It turns out that Lambert's law is inapplicable for most foods prepared in home microwave ovens. Thus, Maxwell's equations must be used to accurately describe the propagation and absorption of radiation.

A common feature, in all these studies is the assumption of constant dielectric and thermal properties. This results in a linear problem, decoupling the wave propagation from the accompanying heat transfer and allowing both phenomena to be analyzed independently. In these works, the transfer of mass is assumed to be unimportant. If significant drying occurs during heating, mass transfer must be accounted for too. A simultaneous heat and mass transfer analysis of drying with microwaves was studied by Wei et al. (1985) with the aid of Lambert's law.

Dielectric properties of most materials vary with tempera-

ture. Foods at frequencies between 400–900 MHz show temperature-sensitive dielectric behavior, but the variation is less pronounced at 2,800 MHz (Ohlsson and Bengtsson, 1975). The rapid change, in the dielectric loss factor during curing, is sometimes used to measure the extent of the cure (Jow et al., 1988). In situations involving a phase transition or during drying, temperature dependence of both the dielectric and thermal properties may influence the process significantly. The change in dielectric properties alters the penetration of radiation, causing uneven temperatures, and sometimes runaway effects. A predictive model then must involve a simultaneous solution of Maxwell's equations with the relevant transport equations.

Transient temperature profiles in plane slabs with temperature-dependent dielectric properties and constant thermal properties have been studied by De Wagter (1984) and Jolly and Turner (1990). De Wagter (1984) deduced the power with the transmission line matrix method, using a network analog of Maxwell's equations. Temperature profiles are predicted using a finite difference discretization and an eigenvector expansion. Jolly and Turner (1990) studied the effect of a fully reflecting support on the heating of a slab of wood exposed to radiation using finite differences. Here, we develop a finite element analysis to simultaneously solve Maxwell's equations with the heat conduction equation for homogeneous multilayered slabs, whose thermal and dielectric properties both vary with temperature. The resulting nonlinear equations are solved by Newton's method. The finite element method is advantageous when analyzing complicated geometries, and in composite media, derivatives of the unknowns at the interfaces can be incorporated in a natural manner. In addition, radiation boundary conditions are used, which restrict the domain of analysis to the sample itself.

The pertinent equations of electromagnetic wave propagation, power dissipation and microwave heating are given in the theory section. Next, the heat equation and Maxwell's equations, with boundary and interface conditions appropriate for composite slabs, are developed. The finite element analysis follows, and lastly applications and conclusions are discussed.

Theory

Wave propagation

A propagating electromagnetic wave is composed of oscillating electric (E) and magnetic (H) field components. Maxwell's equations describing their space and time dependence are

$$\nabla \times E = -\frac{\partial B}{\partial t}$$

and

$$\nabla \times H = J + \frac{\partial D}{\partial t}, \tag{1}$$

where E and H are the electric and magnetic fields, J the current flux, D electric displacement, and B magnetic induction. The constitutive relations relating J, D, and B to E and H are:

$$J = \sigma(\omega)E(t) \quad D = \epsilon(\omega)E(t)$$

and

$$B = \mu(\omega)H(t), \tag{2}$$

where $E = \overline{E}e^{-i\omega t}$ and $H = \overline{H}e^{-i\omega t}$. Alternatively $e^{i\omega t}$ can be used to express the time dependence. Equations 1 and 2 yield:

$$\nabla \times \overline{E} = i\omega\mu(\omega)\overline{H} \tag{3}$$

and

$$\nabla \times \overline{H} = [\sigma(\omega) - i\omega\epsilon(\omega)]\overline{E} \equiv -i\omega\epsilon^*\overline{E}. \tag{4}$$

where the "complex dielectric constant" ϵ^* is defined as:

$$\epsilon^*(\omega) \equiv \epsilon(\omega) + \frac{i\sigma(\omega)}{\omega} \equiv \epsilon'(\omega) + i\epsilon''(\omega). \tag{5}$$

The material's ability to store electrical energy is represented by $\epsilon' = Re(\epsilon^*)$, and $\epsilon'' = Im(\epsilon^*)$ accounts for losses through energy dissipation. The conductivity, $\sigma(\omega)$, dielectric constant, $\epsilon(\omega)$, and the magnetic permeability, $\mu(\omega)$, in general are complex functions of the frequency ω of the radiation.

If magnetic effects are negligible, which is true for most materials used in microwave heating applications, the magnetic permeability $\mu(\omega)$ is well approximated by its value μ_0 in free space. In what follows, we assume this to be true. The material properties are temperature-dependent, thus σ and ϵ in Eq. 2 are the functions of time as well. Since the time scale of electromagnetic propagation is significantly smaller than the time scales for thermal diffusion, an order of magnitude analysis indicates that the terms involving the time derivatives of σ and ϵ are very small and have been neglected. With this assumption and the condition of electroneutrality of the materials considered [which implies $\nabla \cdot (\epsilon\overline{E}) = 0$], Eqs. 3 and 4 can be combined to find:

$$\nabla\left(\overline{E} \cdot \frac{\nabla\epsilon}{\epsilon}\right) + \nabla^2\overline{E} + k^2\overline{E} = 0, \tag{6}$$

where

$$k^2 = \omega^2\mu_0\epsilon_0(\kappa' + i\kappa''). \tag{7}$$

The relative dielectric constant κ' and the relative dielectric loss κ'', are:

$$\kappa' \equiv \epsilon'/\epsilon_0$$

and

$$\kappa'' \equiv \epsilon''/\epsilon_0, \tag{8}$$

To simplify the notation, the overbar on $\overline{E}$ and $\overline{H}$ will be dropped from this point on. The propagation constant k is represented as a complex quantity

$$k = \alpha + i\beta, \tag{9}$$

where α and β are related to the dielectric properties of the

medium and frequency of radiation by:

$$\alpha=\frac{2\pi f}{c}\sqrt{\frac{\kappa'(\sqrt{1+\tan^2\delta}+1)}{2}}, \tag{10}$$

and

$$\beta=\frac{2\pi f}{c}\sqrt{\frac{\kappa'(\sqrt{1+\tan^2\delta}-1)}{2}}, \tag{11}$$

where

$$\tan\delta=\frac{\kappa''}{\kappa'}. \tag{12}$$

In Eqs. 10 and 12, we have used the property $c=1/\sqrt{\mu_0\epsilon_0}$ where c is the speed of light and have replaced ω by $2\pi f$, where f is the frequency of radiation. The phase constant α represents the change of phase of the propagating wave and is related to the wavelength of radiation in the medium (λ_m) by:

$$\lambda_m=\frac{2\pi}{\alpha}, \tag{13}$$

which, in free space, reduces to $\lambda_0=c/f$. The attenuation constant β controls the rate at which the incident field intensity E_0 decays into a sample. For instance, in a semiinfinite sample, the interior field obeys the equation:

$$E=E_0e^{-\beta z}. \tag{14}$$

Thus for higher frequencies, β increases and the penetration of microwaves into the sample decreases. The quantity β^{-1} is known as the characteristic penetration depth, i.e., the distance at which the field intensity decreases to $1/e$ of its incident value.

Power dissipation and Poynting theorem

The power flux associated with a propagating electromagnetic wave is represented by the Poynting vector S and the time average flux for harmonic fields is given by (Stratton, 1941):

$$S=\frac{1}{2}E\times H^*. \tag{15}$$

The Poynting theorem allows the evaluation of the power dissipated in the medium. It is expressed as:

$$\oint_S S\cdot n\,ds=-\frac{1}{2}\omega\epsilon_0\kappa''\int_V E\cdot E^*\,dv + i\omega\int_V\left(\frac{\mu_0}{2}H\cdot H^*+\frac{\epsilon_0\kappa'}{2}E\cdot E^*\right)dv, \tag{16}$$

and states that the net power flow across a surface S enclosing a volume V equals the power dissipated in the medium (real part) to that stored in electric and magnetic fields (imaginary part). Applying the divergence theorem to Eq. 16, the point form of the Poynting theorem is:

$$\nabla\cdot S=-\frac{1}{2}\omega\epsilon_0\kappa''E\cdot E^*+i\omega\left(\frac{\mu_0}{2}H\cdot H^*+\frac{\epsilon_0\kappa'}{2}E\cdot E^*\right), \tag{17}$$

and the power dissipated per unit volume is:

$$p(r)=-Re(\nabla\cdot S)=\frac{1}{2}\omega\epsilon_0\kappa''(E\cdot E^*) \tag{18}$$

Hence, with a knowledge of the electric field intensity in the medium, the local power dissipated is obtained from Eq. 18.

Microwave heating

To obtain transient temperature profiles for a sample exposed to microwave radiation, we solve the heat conduction equation

$$\rho C_p\frac{\partial T}{\partial t}=\nabla\cdot(k\nabla T)+p(r,T), \tag{19}$$

where ρ,C_p, and k are the material density, specific heat capacity and thermal conductivity, respectively. The microwave power, which is a function of the electric field distribution in the medium, is incorporated as a volumetric source term. With appropriate boundary conditions, the solution of Eq. 19 yields transient temperature profiles in objects exposed to the microwave radiation. The dielectric and thermal properties of the medium in general are temperature-dependent, the degree of variation being dependent on the specific application and range of heating. The foregoing analysis is developed for materials whose dielectric and thermal properties are both functions of temperature. Thus, the heat equation, Eq. 19, is coupled to the wave equation, Eq. 6, via the microwave power term.

Analysis

Microwave heating in a composite slab

Consider a slab with m layers of thickness $2L$ exposed to microwaves as shown in Figure 1. The sample is assumed to be homogeneous and isotropic. The surrounding medium is at an ambient temperature during the entire heat-up period, and

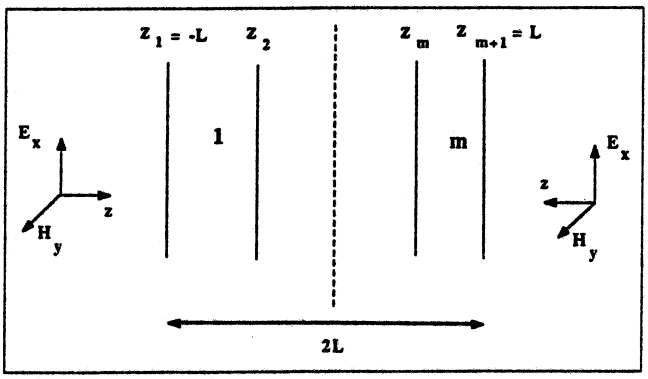

Figure 1. Multilayered sample exposed to plane waves.

heat is lost by convection at the sample boundaries. If ρ_0, $C_{p,0}$, and k_0 are reference thermal properties, then dividing Eq. 19 by k_0 and using the dimensionless variables

$$z_l=\frac{Z_l+L}{2L}, \quad \theta_l=\frac{T_l-T_\infty}{T_0},$$

$$Bi_l=\frac{2h_lL}{k_l}, \quad \tau=\frac{\alpha_0 t}{4L^2},$$

the transient 1*D* heat conduction equation for the multilayer composite is:

$$\overline{\rho_l C_{p,l}}\frac{\partial\theta_l}{\partial\tau}=\frac{\partial}{\partial z}\left(\bar{k}_l\frac{\partial\theta_l}{\partial z}\right)+P_l(z,\theta), \tag{20}$$

for

$$z_l\le z\le z_{l+1}$$

and

$$l=1...m,$$

where

$$P_l=\frac{4p_lL^2}{k_0T_0}, \quad \overline{\rho_l C_{p,l}}=\frac{\rho_l C_{p,l}}{\rho_0,C_{p,0}}$$

and

$$\bar{k}_l=\frac{k_l}{k_0}.$$

The temperature and power, in the lth layer, are θ_l and P_l, respectively. The boundary conditions are

$$\frac{\partial\theta_1}{\partial z}-Bi_1\theta_1=0 \quad \text{at } z=z_1=0,$$

and

$$\frac{\partial\theta_m}{\partial z}+Bi_m\theta_m=0 \quad \text{at } z=z_{m+1}=1. \tag{21}$$

The interface conditions are

$$\left.\begin{aligned}\theta_l&=\theta_{l+1}\\ \bar{k}_l\frac{\partial\theta_l}{\partial z}&=\bar{k}_{l+1}\frac{\partial\theta_{l+1}}{\partial z}\end{aligned}\right\} \quad \begin{aligned}&\text{at} \quad z=z_2...z_m\\ &\text{for} \quad l=1...m-1,\end{aligned} \tag{22}$$

and initial condition

$$\theta_l(\tau=0)=0 \quad \text{for } 0\le z\le 1. \tag{23}$$

The microwave power term is a function of temperature and is obtained by solving Maxwell's equations simultaneously with Eq. 20. The sample is assumed to be at the ambient temperature T_∞, prior to heating.

Maxwell's equations for a composite slab

Microwaves are assumed to be incident normally on the opposite faces of the multilayer slab shown in Figure 1. For propagation of uniform plane waves, the electric and magnetic components lie in a plane $(x-y)$ of uniform intensity varying only in the direction of propagation (z-axis). The wave equation, Eq. 6, then simplifies to:

$$\frac{d^2E_{x,l}}{dZ^2}+k_l^2E_{x,l}=0, \tag{24}$$

for

$$Z_l\le Z\le Z_{l+1} \quad \text{and} \quad l=1...m,$$

where $k_l=\sqrt{\omega^2\mu_0\epsilon_0[\kappa_l'(T)+i\kappa_l''(T)]}$, and $E_{x,l}$, are the propagation constant and electric field intensity in the lth layer, respectively.

In electromagnetic scattering problems a radiation boundary condition is used at a hypothetical boundary surrounding the sample, by satisfying the far field Sommerfield condition (Keller and Givoli, 1989). We want to solve Maxwell's equations for a slab, exposed to radiation of a known intensity, as shown in Figure 1. To avoid having to include the space around the object in the domain for the finite element analysis, radiation boundary conditions, which are applied to the face of the slab, are derived below. For a slab exposed to radiation of intensity E_L from the left, as shown in Figure 1, the solution of Eq. 24 in the space between the object and the source is:

$$E_x(Z)=Ae^{ikZ}+Be^{-ikZ}. \tag{25}$$

If E_L is the intensity of the source from the left,

$$A=E_L, \tag{26}$$

and if $E_x(Z=Z_1)$, it is the intensity at the incident face $Z=Z_1$,

$$B=E_x(Z-Z_1)e^{ikZ_1}-E_Le^{2ikZ_1}. \tag{27}$$

Taking the derivative of Eq. 25 and substituting the expressions for the constants from Eqs. 26 and 27, we get

$$\frac{dE_x}{dZ}+ikE_x=2ikE_Le^{-ikL} \tag{28}$$

at

$$Z=Z_1=-L$$

Similarly, the boundary condition at the face $Z=Z_{m+1}=L$ exposed to radiation of intensity E_R is:

$$\frac{dE_x}{dZ}-ikE_x=-2ikE_Re^{-ikL} \tag{29}$$

A homogeneous boundary condition is obtained, if the face is not exposed to radiation.

From Eq. 3, the relation between the electric and magnetic

field components of the plane wave is:

$$\frac{dE_{x,l}}{dZ} = i\mu_0\omega H_{y,l}\,. \tag{30}$$

The interface conditions for the electric and magnetic field vectors are:

$$\left.\begin{aligned} n\times(E_l - E_{l+1}) &= 0 \\ n\times(H_l - H_{l+1}) &= 0 \end{aligned}\right\} \quad \begin{aligned} &\text{at} \quad Z = Z_2 \ldots Z_m \\ &\text{and} \quad l = 1 \ldots m-1. \end{aligned} \tag{31}$$

For the case of uniform plane waves propagating in the z direction, by substituting Eq. 30 into Eq. 31 and simplifying, we get

$$\left.\begin{aligned} E_{x,l} &= E_{x,l+1} \\ \frac{\partial E_{x,l}}{\partial Z} &= \frac{\partial E_{x,l+1}}{\partial Z} \end{aligned}\right\} \quad \begin{aligned} &\text{at} \quad Z = Z_2 \ldots Z_m \\ &\text{and} \quad l = 1 \ldots m-1. \end{aligned} \tag{32}$$

Finite element analysis

To incorporate Eq. 24 with the unknown complex electric field E into the finite element analysis, equations involving the real and imaginary components and their boundary conditions are developed. If the intensity of the electric field incident from the left is E_L, then using the dimensionless variables

$$u_{x,l} = \frac{E_{x,l}}{E_L} \quad \text{and} \quad z_l = \frac{Z_l + L}{2L}\,,$$

Eq. 24 simplifies to

$$\frac{d^2u_{x,l}}{dz^2} + \gamma_l^2 u_{x,l} = 0, \tag{33}$$

for

$$z_l \le z \le z_{l+1} \quad \text{and} \quad l = 1 \ldots m,$$

where $\gamma_l = \sqrt{4L^2\omega^2\mu_0\epsilon_0[\kappa_l'(\theta) + i\kappa_l''(\theta)]}$, and $u_{x,l}$, are the propagation constant and electric field intensity in the lth layer, respectively. The field variable, $u_{x,l}$, is a complex quantity. For the finite element analysis, the field equation, Eq. 33, is reduced to two equations involving the real and imaginary components. Substituting, $u_{x,l} = v_{x,l} + iw_{x,l}$, into Eq. 33 and equating the real and imaginary components, we get:

$$\frac{d^2v_{x,l}}{dz^2} + \psi_l v_{x,l} - \chi_l w_{x,l} = 0 \tag{34}$$

and

$$\frac{d^2w_{x,l}}{dz^2} + \chi_l v_{x,l} + \psi_l w_{x,l} = 0, \tag{35}$$

for

$$z_l \le z \le z_{l+1} \quad \text{and} \quad l = 1 \ldots m,$$

where $\psi_l = 4L^2\omega^2\mu_0\epsilon_0\kappa_l'(\theta)$ and $\chi_l = 4L^2\omega^2\mu_0\epsilon_0\kappa_l''(\theta)$.

The boundary conditions for the real and imaginary components from Eqs. 28 and 29 are:

$$\left.\begin{aligned} \frac{dv_{x,1}}{dz} - 2\alpha_0 L w_{x,1} &= 4\alpha_0 L\sin(\alpha_0 L) \\ \frac{dw_{x,1}}{dz} + 2\alpha_0 L v_{x,1} &= 4\alpha_0 L\cos(\alpha_0 L) \end{aligned}\right\} \quad \text{at } z = 0 \tag{36}$$

and

$$\left.\begin{aligned} \frac{dv_{x,m}}{dz} + 2\alpha_0 L w_{x,m} &= -4\frac{E_R}{E_L}\alpha_0 L\sin(\alpha_0 L) \\ \frac{dw_{x,m}}{dz} - 2\alpha_0 L v_{x,m} &= -4\frac{E_R}{E_L}\alpha_0 L\cos(\alpha_0 L) \end{aligned}\right\} \quad \text{at } z = 1. \tag{37}$$

The interface conditions from Eq. 32 for the component $v_{x,l}$, are:

$$\left.\begin{aligned} v_{x,l} &= v_{x,l+1} \\ \frac{\partial v_{x,l}}{\partial z} &= \frac{\partial v_{x,l+1}}{\partial z} \end{aligned}\right\} \quad \begin{aligned} &\text{at} \quad z = z_2 \ldots z_m \\ &\text{and} \quad l = 1 \ldots m-1. \end{aligned} \tag{38}$$

Similar interface conditions hold for the component $w_{x,l}$.

The expression for the microwave power term in Eq. 20 is:

$$P_l(z,\theta) = \frac{2L^2\omega\epsilon_0\kappa_l''(\theta)E_L^2}{k_0T_0}\,(v_{x,l}^2 + w_{x,l}^2), \tag{39}$$

for

$$z_l \le z \le z_{l+1} \quad \text{and} \quad l = 1 \ldots m.$$

The Galerkin finite element method is used to solve the coupled nonlinear equations (Eqs. 20, 34 and 35) with their respective interface and boundary conditions. For a general equation of the form:

$$Ly = f, \tag{40}$$

Galerkin finite elements consist of expanding the unknown, u, in a finite element basis set $\{\phi\}$. Thus,

$$u \approx \tilde{u} = \sum_{j=1}^{N} y_j\phi_j(z). \tag{41}$$

The error, $L\tilde{u} - f$, is set orthogonal to the basis functions, and

$$\int_0^1 (L\tilde{u} - f)\phi_i\,dz = 0, \tag{42}$$

for

$$i = 1 \ldots N.$$

Integrating by parts, and incorporating boundary and interface

conditions, Eq. 42 results in a set of algebraic equations whose solution yields the unknown coefficients, y_j, of the expansion.

Expanding the real (v_x) and imaginary components (w_x) of the electric field, and the temperature (θ) in the basis $\{\phi\}$,

$$\tilde{v}_x=\sum_{k=1}^{N} v_k\phi_k(z), \quad \tilde{w}_x=\sum_{k=1}^{N} w_k\phi_k(z)$$

and

$$\tilde{\theta}=\sum_{k=1}^{N}\theta_k(\tau)\phi_k(z) \tag{43}$$

for

$$0\le z\le 1,$$

the Galerkin finite element method yields the following nonlinear residual equations for Eqs. 34, 35 and 20, respectively.

$$R_i^{(1)}=\sum_{k=1}^{N} v_k^{t+1}\int_0^1\phi_i'\phi_k'dz-\sum_{k=1}^{N} v_k^{t+1}\int_0^1\psi(\theta^{t+1})\phi_i\phi_k dz$$
$$+\sum_{k=1}^{N} w_k^{t+1}\int_0^1\chi(\theta^{t+1})\phi_i\phi_k dz+2L\alpha_0 w_1^{t+1}\delta_{i1}+4L\alpha_0\sin\alpha_0 L\delta_{i1}$$
$$+2L\alpha_0 w_N^{t+1}\delta_{iN}+4\frac{E_R}{E_L}L\alpha_0\sin\alpha_0 L\delta_{iN} \tag{44}$$

$$R_i^{(2)}=\sum_{k=1}^{N} w_k^{t+1}\int_0^1\phi_i\phi_k dz-\sum_{k=1}^{N} v_k^{t+1}\int_0^1\chi(\theta^{t+1})\phi_i\phi_k dz$$
$$-\sum_{k=1}^{N} w_k^{t+1}\int_0^1\psi(\theta^{t+1})\phi_i\phi_k dz-2L\alpha_0 v_1^{t+1}\delta_{i1}+4L\alpha_0\cos\alpha_0 L\delta_{i1}$$
$$-2L\alpha_0 v_N^{t+1}\delta_{iN}+4\frac{E_R}{E_L}L\alpha_0\cos\alpha_0 L\delta_{iN} \tag{45}$$

$$R_i^{(3)}=\sum_{k=1}^{N}\int_0^1 f(\overline{\rho C_p}^{t+1})\left\{\frac{\theta_k^{t+1}-\theta_k^t}{\Delta\tau}\right\}\phi_i\phi_k dz$$
$$+\sum_{k=1}^{N}\theta_k^{t+1}\int_0^1 f(\bar{k}^{t+1})\phi_i'\phi_k' dz-\frac{2L^2\omega\epsilon_0 E_L^2}{k_0T_0}\int_0^1\kappa''(\theta^{t+1})$$
$$\times\left\{\left(\sum_k v_k^{t+1}\phi_k\right)^2+\left(\sum_k w_k^{t+1}\phi_k\right)^2\right\}\phi_i dz+\bar{k}_1(\theta^{t+1})Bi_1(\theta^{t+1})\theta_1^{t+1}\delta_{i1}$$
$$+\bar{k}_m(\theta^{t+1})Bi_m(\theta^{t+1})\theta_N^{t+1}\delta_{iN} \tag{46}$$

where

$$\left.\begin{aligned}\kappa''(\theta)&=\kappa_l''(\theta)\\ \kappa'(\theta)&=\kappa_l'(\theta)\\ f(\overline{\rho C_p})&=\frac{\rho_l(\theta)C_{p,l}(\theta)}{\rho_0 C_{p,0}}\\ f(\bar{k})&=\frac{k_l(\theta)}{k_0}\end{aligned}\right\}\quad \begin{aligned}z_l\le z\le z_{l+1}\\ l=1\ldots m\end{aligned} \tag{47}$$

and

$$i=1\ldots N \quad \text{and} \quad t=\text{time index}$$

An implicit backward difference, is used to discretize the time domain and results in an unconditionally stable algorithm. The residuals equations (Eqs. 44, 45 and 46) result in a set of nonlinear algebraic equations that are solved using a Newton-Raphson scheme to determine the coefficients of the expansions in Eq. 43 at each time step. The power in each layer is then deduced from Eq. 18. At each time step, the linear ($3N\times 3N$) system solved is:

$$J(u^{n,t+1})[u^{n,t+1}-u^{n+1,t+1}]=R(u^{n,t+1}) \tag{48}$$

$$n-\text{Newton iterate index} \quad t-\text{time index}$$

where

$$J=\begin{pmatrix}\frac{\partial R_i^{(1)}}{\partial v_j} & \frac{\partial R_i^{(1)}}{\partial w_j} & \frac{\partial R_i^{(1)}}{\partial \theta_j}\\ \cdots & \cdots & \cdots\\ \frac{\partial R_i^{(2)}}{\partial v_j} & \frac{\partial R_i^{(2)}}{\partial w_j} & \frac{\partial R_i^{(2)}}{\partial \theta_j}\\ \cdots & \cdots & \cdots\\ \frac{\partial R_i^{(3)}}{\partial v_j} & \frac{\partial R_i^{(3)}}{\partial w_j} & \frac{\partial R_i^{(3)}}{\partial \theta_j}\end{pmatrix} \qquad u^{n,t+1}=\begin{pmatrix}v_1^{n,t+1}\\ \vdots\\ v_N^{n,t+1}\\ w_1^{n,t+1}\\ \vdots\\ w_N^{n,t+1}\\ \theta_1^{n,t+1}\\ \vdots\\ \theta_N^{n,t+1}\end{pmatrix}$$

and

Table 1. Dielectric Constant κ' Data (Ohlsson and Bengtsson, 1975): $\kappa'=a_0+a_1T+a_2T^2+a_3T^3$ (T Kelvin)

Material	f(MHz)	a_0	a_1	a_2	a_3
Pizza-baked dough	2,800	4.6			
Pizza-baked dough	2,800	−3.7022	2.6×10^{-2}		
Ground beef	2,800	44.1			
Raw beef	450	1,061.8	−7.7019	1.935×10^{-2}	-1.6204×10^{-5}
Raw beef	900	82.23	−0.1059		
Raw beef	2,800	−552.64	5.2189	-1.4991×10^{-2}	1.412×10^{-5}
Ham	2,800	−917.03	5.0859	-6.32×10^{-3}	
Nylon (Huang, 1976)	3,000	16.727	−0.10279	2.4192×10^{-4}	-1.7592×10^{-7}

Table 2. Dielectric Loss κ'' Data (Ohlsson and Bengtsson, 1975): $\kappa'' = b_0 + b_1 T + b_2 T^2 + b_3 T^3 + b_4 T^4$ (T Kelvin)

Material	f(MHz)	b_0	b_1	b_2	b_3	b_4
Pizza-baked dough	2,800	0.6				
Pizza-baked dough	2,800	−1.297	5.6×10^{-3}			
Ground beef	2,800	11.3				
Raw beef	450	−199.09	0.8171			
Raw beef	900	236.85	−1.527	2.7277×10^{-3}		
Raw beef	2,800	332.66	−2.6032	6.9321×10^{-3}	-6.0185×10^{-6}	
Ham	2,800	−378.85	2.2237	-2.8×10^{-3}		
Nylon (Huang, 1976)	3,000	84.16	−1.0011	4.4563×10^{-3}	-8.8029×10^{-6}	6.5208×10^{-9}

Table 3. Thermal Data for Calculations*

Material	k(W·m^{-2}·K^{-1})	ρ(kg·m^{-3})	C_p(J·kg^{-1}·K^{-1})
Pizza-baked dough	0.45	800	2,850
Nyon (Brandrup et al., 1989)	0.43	1,200	$349.02+0.4738T$

*Temperature Dependence of Thermal Properties of Raw Beef and Ham were assumed to be those of water (Welty et al., 1984).

$$R^{n,t+1} = \begin{pmatrix} R_1^{(1)}(u^{n,t+1}) \\ \vdots \\ R_N^{(1)}(u^{n,t+1}) \\ R_1^{(2)}(u^{n,t+1}) \\ \vdots \\ R_N^{(2)}(u^{n,t+1}) \\ R_1^{(3)}(u^{n,t+1}) \\ \vdots \\ R_N^{(3)}(u^{n,t+1}) \end{pmatrix} \quad \begin{matrix} i=1\ldots N \\ \\ j=1\ldots N \end{matrix}$$

Continuity of temperature at interfaces between two materials is imposed by placing an element node at the interface. Due to lack of a good initial guess to begin the Newton scheme, a very small time step ($\Delta t = 1\times10^{-4}$ s) was used. Quadratic basis functions with three nodes per element and 10–15 elements were used.

Results and Discussion

The numerical method is illustrated with applications to the microwave heating of foods and polymers. Tabulated dielectric and thermal data from the literature, over the temperature range of interest, were fitted to polynomials using a least-squares method. These polynomials were used to represent the temperature-dependent functions given in Eq. 47. The properties and the polynomials used in the calculations are listed in Tables 1, 2 and 3 with the literature sources. Temperature dependence of fresh meats parallels those of water (Sweat, 1986). Thus, we have used the heat transfer properties of water for the calculations involving raw beef and ham.

The flux of incident radiation, I_0, in free space, is related to the electric field intensity E, by

$$I_0 = \frac{1}{2} c\epsilon_0 E^2. \tag{49}$$

Equation 49 was used to deduce the intensity of incident electric field for a given intensity of radiation. The value of the heat transfer coefficient, h, was chosen to be 2 $W\cdot m^{-2}\cdot K^{-1}$.

To check the validity of the finite element solution to Maxwell's equations in a multilayer sample with the radiation boundary condition, we have compared it with the analytic solution for a sample with constant dielectric properties. Figure 2 is a composite made of 2-*cm*-thick outer layers of pizza-baked dough, and a 1-*cm* central layer of ground beef. The numerical solution is within the linewidth of the analytical solution.

Power distributions and transient temperature profiles are shown for a slab of raw beef exposed to microwaves of equal intensity on both faces, in Figures 3, 4 and 5. At the lower frequencies of 450 MHz and 900 MHz, dielectric properties are strong functions of temperature. Penetration depths for both samples shown as insets in Figures 3 and 4 decrease with

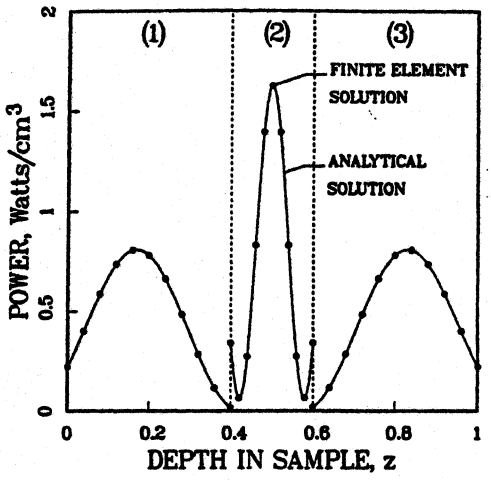

Figure 2. Finite element solution of Maxwell's equations with the analytical solution for constant dielectric properties.

(1) Pizza-baked dough, (2) ground beef, (3) pizza-baked dough $2L = 5$ *cm*, $f = 2{,}800$ MHz, $I_{0,L} = I_{0,R} = 3$ $W\cdot cm^{-2}$

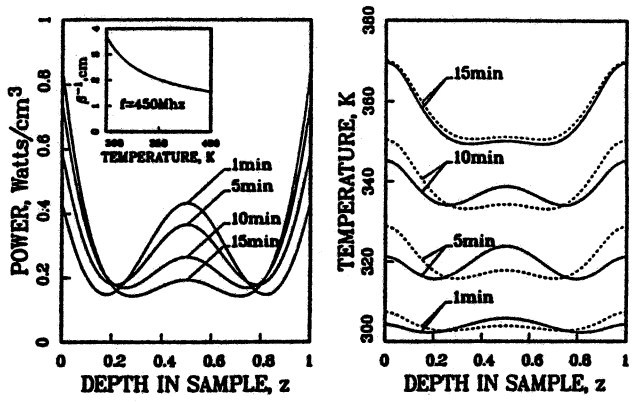

Figure 3. Power and temperature distributions for a raw beef sample exposed to microwaves.

- - - , constant dielectric properties
$2L = 5.5$ cm, $f = 450$ MHz, $I_{0,L} = I_{0,R} = 3$ W·cm^{-2}

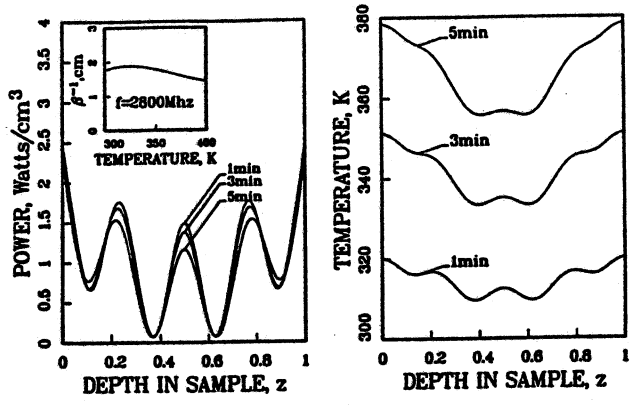

Figure 5. Power and temperature distributions for a raw beef sample exposed to microwaves.

$2L = 3$ cm, $f = 2{,}800$ MHz, $I_{0,L} = I_{0,R} = 3$ W·cm^{-2}

increased temperatures. Thus, at the onset of heating, the sample appears thinner to the radiation, and the microwaves from opposite faces interfere to produce the peak in the center of the slab. As heating proceeds, two main features are observed. Due to the decrease in penetration depth, the microwaves decay into the sample without significant penetration. The increasing dielectric loss factor, however, causes the face temperature to rise sharply, resulting in very uneven temperature distributions as seen in Figure 3 after 15 min of heating. In Figure 4, the power is highly peaked in the center at the onset of heating. As heating proceeds, the power deposition and temperatures in the center of the slab rise, as the increase in dielectric loss dominates over the influence of decreasing penetration. At later times, the decrease in penetration depth controls, and the temperature at the center decreases. In Figures 4 and 5, the temperature profiles are compared with the heating patterns predicted with constant dielectric properties.

At 2,800 MHz, dielectric properties are only weakly dependent on temperature. This is evident in Figure 5, where the power distribution changes only slightly as the sample heats. Thus, for the raw beef modeled here, the temperature dependence of dielectric properties is not very important for cooking in a typical home microwave oven (2,450 MHz).

Figure 6 illustrates a runaway heating effect. The sharp rise in the dielectric loss factor with temperature for Nylon 66 causes a sudden increase in temperature at the center of the slab, during the 5th minute of heating. Such a situation can lead to hot spots in a very short time yielding very uneven temperature profiles in the sample. Figure 7 is a multilayer sample of pizza-baked dough and ham arranged as shown and illuminated from the left face with radiation of frequency 2,800 MHz. The outer layers have dielectric properties that are weak functions of temperature.

Conclusion

We developed a finite element solution to simultaneously solve Maxwell's equations with the heat equation for multilayer slabs and with temperature-dependent thermal and dielectric properties exposed to plane waves. By using the radiation boundary condition at the face of the sample, the knowledge of intensity of the incident radiation is sufficient to describe the wave propagation within the medium. An important effect accompanying increasing loss tangents is the decreasing penetration of microwaves as the sample heats. Thus, the sample

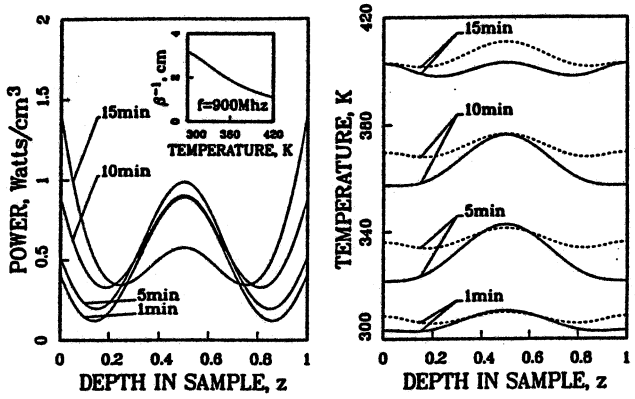

Figure 4. Power and temperature distributions for a raw beef sample exposed to microwaves.

- - - , constant dielectric properties
$2L = 3$ cm, $f = 900$ MHz, $I_{0,L} = I_{0,R} = 3$ W·cm^{-2}

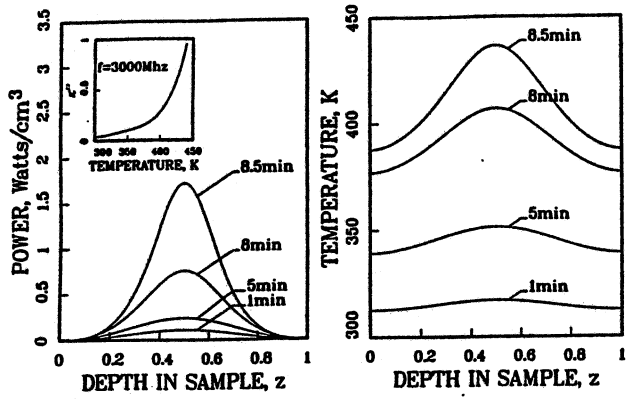

Figure 6. Power and temperature distributions for Nylon 66 exposed to microwaves.

$2L = 3$ cm, $f = 3{,}000$ MHz, $I_{0,L} = I_{0,R} = 3$ W·cm^{-2}

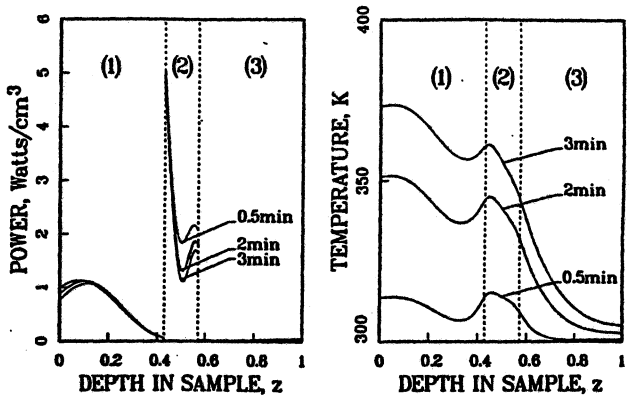

Figure 7. Power and temperature distributions for a multilayered slab.

(1) Pizza-baked dough, (2) ham, (3) pizza-baked dough
$2L = 3.5$ cm, $f = 2{,}800$ MHz, $I_{0,L} = 3$ W·cm^{-2}, $I_{0,R} = 0$

appears thicker to the radiation as its temperature rises. This further accentuates the rise of temperatures at the face of the sample due to the higher dielectric loss factor. The model is useful in predicting runaway heating effects during microwave processing, where uniformity of temperature is essential to the quality of the product.

Acknowledgment

We thank Kraft General Foods Inc. for financial support and the Minnesota Supercomputer Institute for computing resources.

Notation

B = magnetic induction, Wb·m^{-2}
Bi = Biot number
c = velocity of light, m·s^{-1}
C_p = specific heat capacity, J·kg^{-1}·K^{-1}
$C_{p,o}$ = reference specific heat capacity, J·kg^{-1}·K^{-1}
D = electric displacement, C·m^{-2}
E = electric field intensity V·m^{-1}
f = frequency of incident radiation, Hz
h = heat transfer coefficient, W·m^{-2}·K^{-1}
H = magnetic field intensity, Amp·m^{-1}
J = current flux, Amp·m^{-2}
k = thermal conductivity, W·m^{-1}·K^{-1}
k_0 = reference thermal conductivity, W·m^{-1}·K^{-1}
L = half length of sample, m
p = microwave source term, W·m^{-3}
P = dimensionless microwave source term
S = Poynting vector, W·m^{-2}
t = time, s
T = temperature, K
T_∞ = ambient temperature, K
T_o = initial temperature, K
u = dimensionless electric field intensity
v = dimensionless real field component
w = dimensionless imaginary field component
z = dimensionless distance
Z = distance, m

Greek letters

α = wave number, m^{-1}
α_o = reference thermal diffusivity, m^2·s^{-1}
α_0 = free space wave number, m^{-1}
β = attenuation constant, m^{-1}
γ = propagation constant
δ = kronecker delta
ϵ = permittivity, Farad·m^{-1}
ϵ_0 = free space permittivity, Farad·m^{-1}
ϵ' = dielectric constant, Farad·m^{-1}
ϵ'' = dielectric loss factor, Farad·m^{-1}
θ = dimensionless temperature
κ = relative permittivity
κ' = relative dielectric constant
κ'' = relative dielectric loss
λ = wavelength, m
μ = permeability, Henry·m^{-1}
μ_0 = free space permeability Henry·m^{-1}
ρ = density, kg·m^{-3}
ρ_0 = reference density, kg·m^{-3}
σ = electric conductivity, mho·m^{-1}
τ = dimensionless time
ϕ = basis functions
ω = angular frequency, Rad·s^{-1}

Subscripts

l = layer
L = incidence from left
m = number of layers in composite
R = incidence from right

Superscripts

n = newton iterate index
t = time index

Literature Cited

Ayappa, K. G., H. T. Davis, G. Crapiste, E. A. Davis, and J. Gordon, "Microwave Heating: an Evaluation of Power Formulations," *Chem. Eng. Sci.*, in press (1990).

Brandrup, J., and E. H. Immergut, *Polymer Handbook*, 3rd ed., Wiley, New York (1989).

Chan, A. K., R. A. Sigelmann, A. W. Guy, and J. F. Lehmann, "Calculation by Method of Finite Difference of the Temperature Distribution in Layered Tissues," *IEEE Trans. Biomed. Eng. BME*, **20**, 86 (1973).

Chabinsky, I. J., "Applications of Microwave Energy: Past, Present, and Future Brave New World," *Mat. Res. Symp. Proc.*, **124**, 17 (1988).

Datta, A. K., "Heat and Mass Transfer in the Microwave Processing of Food," *Chem. Eng. Prog.*, **6**, 47 (1990).

De Wagter, C., "Computer Simulation Predicting Temperature Distributions Generated by Microwave Absorption in Multilayered Media," *J. Microwave Power*, **19**, 97 (1984).

Durney, C. H., "Electromagnetic Dosimetry for Models of Humans and Animals: a Review of Theoretical and Numerical Techniques, *Proc. IEEE*, **68**, 33 (1980).

Guy, A. W., "Electromagnetic Fields and Relative Heating Patterns Due to a Rectangular Aperture Source in Direct Contact with Bilayered Biological Tissue," *IEEE Trans. MTT*, **19**, 214 (1971).

Huang, H., "Temperature Control in a Microwave Resonant Cavity System for Rapid Heating of Nylon Monofilament," *J. Microwave Power*, **11**, 305 (1976).

Jolly, P., and I. Turner, "Non-Linear Field Solutions of One-Dimensional Microwave Heating," *J. Microwave Power and EM Energy*, **25**, 3 (1990).

Jow, J., M. C. Hawley, M. Finzel, and T. Kern, "Dielectric Analysis of Epoxy/Amine Resins Using Microwave Cavity Technique," *Polymer Eng. and Sci.*, **28**, 1450 (1988).

Keller, J. B., and D. Givoli, "Exact Non-Reflecting Boundary Conditions," *J. Comp. Phys.*, **82**, 172 (1989).

Le Van, Q., and A. Gourdenne, "Microwave Curing of Epoxy Resins with Diaminodiphenylmethane: i. General Features," *Eur. Polym. J.*, **23**, 777 (1987).

Livesay, D. E. and K. Chen, "Electromagnetic Fields Induced Inside Arbitrarily Shaped Biological Bodies," *IEEE Trans. Microwave Theory Tech. MTT*, **22**, 1273 (1974).

Lynch, D. R., K. D. Paulsen, and J. W. Strohbehn, "Finite Element Solution of Maxwell's Equations for Hyperthermia Treatment Planning," *J. of Comput. Phys.*, **58**, 246 (1985).

Malaczynski, G. W., "Adhesive Processing by Electromagnetic Irradiation," *Polym. Eng. and Sci.*, **28**, 1270 (1988).
Mandal, S., T. Sundararajan, and P. S. Ghoshdastidar, "A Coupled Analysis of Thermal and Electromagnetic Phenomena during Hyperthermia in Biological Tissues," *Bioheat Transfer: Applications in Hyperthermia, Emerging Horizons in Instrumentation and Modeling*, ASME Meeting, **126**, 59 (1989).
Neuder, S. M., "Electromagnetic Fields in Biological Media: 2. the SCAT Program Multilayered, Spheres, Theory and Applications," *U.S. Dept. of Health Education, and Welfare (FDA)*, **79-8072** (1979).
Nykvist, W. E., and R. V. Decareau, "Microwave Meat Roasting," *J. Microwave Power*, **11**, 3 (1976).
Ohlsson, T., and N. E. Bengtsson, "Microwave Heating Profiles in Foods: a Comparison between Heating Experiments and Computer Simulation," *Microwave Energy Appl. Newsletter*, **6**, 3 (1971).
Ohlsson, T., and N. E. Bengtsson, "Dielectric Food Data for Microwave Sterilization," *J. Microwave Power*, **10**, 93 (1975).
Schwan, H. P., E. L. Cartensen, and L. Kam, "Heating of Fat-Muscle Layers by Electromagnetic and Ultrasonic Diathermy," *Trans. AIEE. Comm. and Electronics*, **9**, 483 (1953).
Schwan, H. P., and K. Li, "Hazards Due to Total Body Irradiation by Radar," *Proc. of IRE*, **11**, 1572 (1956).
Spiegel, R. J., "A Review of Numerical Models for Predicting the Energy Deposition and Resultant Thermal Response of Humans Exposed to Electromagnetic Fields," *IEEE Trans. Microwave Theory Tech. MTT*, **32**, 730 (1984).
Stratton, J. A., *Electromagnetic Theory*, McGraw-Hill, New York (1941).
Stuchly, S. S., and M. A. K. Hamid, "Physical Parameters in Microwave Heating Processes," *J. Microwave Power*, **7**, 117 (1972).
Sweat, V. E., "Thermal Properties of Foods," *Engineering Properties of Foods*, M. A. Rao and S. S. H. Rizvi, eds., 49 (1986).
Taoukis, P., E. A. Davis, H. T. Davis, J. Gordon, and Y. Talmon, "Mathematical Modeling of Microwave Thawing by the Modified Isotherm Migration Method," *J. Food Sci.*, **52**, 455 (1987).
Taflove, A., and M. E. Brodwin, "Computation of the Electromagnetic Fields and Induced Temperatures Within a Model of the Microwave Irradiated Human Eye," *IEEE Trans. Microwave Theory Tech. MTT*, **23**, 888 (1975).
Wei, C. K., Davis, H. T., E. A. Davis, and J. Gordon, "Heat and Mass Transfer in Water Laden Sandstone: Microwave Heating," *AIChE J.*, **31**, 842 (1985).
Weil, C. M., "Absorption Characteristics of Multilayered Sphere Models Exposed to UHF/Microwave Radiation," *IEEE. Trans. on BME*, **22**, 468 (1975).
Welty, J. R., C. E. Wicks, and R. E. Wilson, *Fundamentals of Momentum, Heat and Mass Transfer*, 3rd ed., Wiley, New York (1984).

Manuscript received Aug. 7, 1990, and revision received Jan. 8, 1991.